The Nonlinear Pathway of Y Ganglion Cells in the Cat Retina

JONATHAN D. VICTOR and ROBERT M. SHAPLEY

From The Rockefeller University, New York 10021

ABSTRACT Retinal ganglion cells of the Y type in the cat retina produce two different types of response: linear and nonlinear. The nonlinear responses are generated by a separate and independent nonlinear pathway. The functional connectivity in this pathway is analyzed here by comparing the observed second-order frequency responses of Y cells with predictions of a "sandwich model" in which a static nonlinear stage is sandwiched between two linear filters. The model agrees well with the qualitative and quantitative features of the second-order responses. The prefilter in the model may well be the bipolar cells and the nonlinearity and postfilter in the model are probably associated with amacrine cells.

INTRODUCTION

The ganglion cells of the cat retina may be classified by the major qualitative features of their response to modulated patterns of light (Enroth-Cugell and Robson, 1966). The X cells respond to fine patterns in a qualitatively linear way, whereas the response of Y cells to such patterns is nonlinear. The purpose of this paper is to provide a concise model of the spatial and temporal structure of the distinctive nonlinear pathway of the Y cell. The form of the model suggests a natural correspondence of the model with retinal anatomy. Nonlinear systems are in general more complex than linear systems but they do offer one advantage. Because the sequence of transductions in a nonlinear system matters, one can infer this sequence from input-output studies (Spekreijse, 1969). We have exploited this advantage in the work reported here, in order to establish the sequence of transductions in the nonlinear pathway of the cat retina.

It has already been established that Y ganglion cells possess a duplex receptive field organization. Such cells have a "linear" receptive field center and a "linear" surround mechanism, but also receive input from another receptive field mechanism, the nonlinear subunits (Hochstein and Shapley, 1976 *b*; Victor and Shapley, 1979). The nonlinear subunits give rise to the characteristic even-order nonlinear responses of Y cells, for instance, frequency-doubling and second-order intermodulation. In this paper we present observations of the dynamics of the nonlinear subunit mechanism, and the theoretical consequences of such observations. The simplest kind of theoretical

J. GEN. PHYSIOL. © The Rockefeller University Press · 0022-1295/79/12/0671/19 $1.00 671
Volume 74 December 1979 671-689

model that includes spatial integration within a subunit, then a nonlinear transduction, and then pooling of subunit signals, is a model we refer to as a linear/nonlinear/linear sandwich model. We will show that a linear/nonlinear/linear "sandwich" model accounts for the dynamic properties of the nonlinear responses of Y cells. We have also measured the dependence of the nonlinear responses on spatial pattern and contrast. These results allow us to infer the physiological and anatomical identities of components of the "sandwich" model.

METHODS

Our procedures for recording the responses of retinal ganglion cells, producing visual stimuli, and analyzing the resultant impulse trains have been described previously (Victor and Shapley, 1979). We summarize these methods below.

Physiological Preparation

Recordings were made from single optic tract fibers of anaesthetized paralyzed adult cats. During recording, cats were anaesthetized with urethane and paralyzed with a gallamine triethiodide/diallylbis-(nortoxiferine) mixture.

Contact lenses with a +2D correction and a 3-mm artificial pupil were affixed to both eyes. Optic discs were mapped on a tangent screen with a hand-held ophthalmoscope. If necessary, optics were corrected with spectacle lenses to be in focus at 57 cm, the distance of the visual stimulus.

Units were classified as X and Y by their response to contrast reversal of a just-resolvable luminance grating (Hochstein and Shapley, 1976 *a*). After classification, Y cells were studied quantitatively as described below. The data presented below are based on responses of 93 Y cells (67 on-center, 26 off-center).

Visual Stimuli

Patterned visual stimuli were generated on a cathode ray tube (Hewlett-Packard Co., Palo Alto, Calif., model 1321A). The display subtended a visual angle of 20° × 20° at a distance of 57 cm. The mean luminance of the display was 20 cd/m^2. The control voltages for the cathode ray tube were produced by specialized electronic circuitry (Shapley and Rossetto, 1976). The frame rate of the display was 200 Hz, and there were 900 vertical raster lines in the display. A pattern wave form synchronized to the horizontal input was multiplied in an analog multiplier by a temporal modulation signal that was slow in comparison to the frame rate. The resulting spatiotemporal product was fed to the intensity input of the display. A temporal modulation signal of zero produced a uniform display at the mean luminance. A negative temporal modulation signal reversed the contrast of the spatial pattern. For classifying units, a 2-Hz square wave constituted the temporal modulation signal. For quantitative analysis of Y cell responses, the temporal modulation signal was a computer-generated sum of sinusoids.

In these experiments, the sum-of-sinusoids signal had eight component sinusoids; the frequency f_j of the jth sinusoid was $(2^{j+2} - 1)/32.768$ Hz. Thus, the eight frequencies were 0.214, 0.458, 0.946, 1.923, 3.876, 7.782, 15.594, and 31.219 Hz.

Data Collection and Analysis

A computer collected the occurrence times of neural impulses elicited by sum-of-sinusoids modulation of a spatial pattern. For each spatial pattern, the temporal

modulation signal was routinely presented at four contrasts: 0.0125, 0.025, 0.05, and 0.10 per sinusoid. 5 s elapsed between the onset of each contrast level and the beginning of data collection. Each contrast level was presented for eight episodes of 40 s, and episodes with different contrast levels were interleaved. The temporal modulation signal used at a given contrast level was

$$s(t) = a \sum_{j=1}^{8} \sin [2\pi(f_j t)]. \quad (1)$$

The first-order frequency kernel K_1 (F) consists of Fourier components of the impulse train at the frequency f_j in the input signal:

$$K_1(f_j) = 2\langle r(t) \cdot e^{-2\pi i(f_j t)} \rangle. \quad (2)$$

In this equation, $r(t)$ denotes the response of the neuron, which is treated as a train of delta functions. The brackets denote an average over time. The first-order frequency kernel (Eq. 2) is essentially the transfer function of the linear transducer that best approximates the transduction under study, and is thus a generalization of the transfer function of a linear transduction. To be explicit, the transduction we are considering is that from luminance to probability of impulse firing by the ganglion cell.

The second-order frequency kernel $K_2(F_1, F_2)$ consists of Fourier components of the impulse train at pairwise combination frequencies $f_j \pm f_k$ of frequencies in the input signal:

$$K_2(f_j, \pm f_k) = 2\langle r(t) \cdot e^{-2\pi i(f_j \pm f_k)t} \rangle \; j \neq k$$

$$K_2(f_j, f_j) = 4\langle r(t) \cdot e^{-2\pi i(2f_j t)} \rangle. \quad (3)$$

On successive repeats of each contrast level, the relative phases of the input sinusoids were varied. Thus, the averaging process of Eqs. 2 and 3 extends over input phase, as well as time. This removed fourth (and perhaps higher) even-order interactions from the measured second-order frequency kernel (Victor and Shapley, 1980).

The frequency kernels $K_1(F)$ and $K_2(F_1, F_2)$ are viewed as continuous functions of their arguments. The sum-of-sinusoids technique provides an estimate of these functions at the mesh of frequencies present in the input ensemble. The frequency kernels were calculated off-line on a PDP 11/45 computer (Digital Equipment Corp., Marlboro, Mass.). The experimental measurements of $K_1(f_j)$ and $K_2(f_j, \pm f_k)$ at a discrete lattice of points were interpolated to form smooth functions $K_1(F)$ and $K_2(F_1, F_2)$ by a standard cubic spline (Ahlberg et al., 1967). The amplitude of the first-order frequency kernel, which is a function of one variable, is displayed on a log-log plot. The amplitude of the second-order frequency kernel, which is a function of two variables, is displayed as a contour map. For further details on the sum-of-sinusoids procedure and theoretical background, see Victor and Shapley (1979, 1980) and Victor and Knight (1979).

RESULTS

First, we show that the Y cell nonlinear response is generated locally in the receptive field. This leads to a "sandwich model" for the nonlinear pathway. Then, the dynamics of the nonlinear pathway are analyzed. Finally, we consider the spatial characteristics and contrast dependence of the components of the sandwich model.

Local Generation of the Nonlinear Response

The response of a Y cell to gratings of low spatial frequency contains both first- and second-order components (Victor and Shapley, 1979). The sum-of-sinusoids technique has provided strong evidence for the independence of the first- and second-order responses (Victor et al., 1977). The response of a Y cell to a low spatial frequency luminance grating modulated by a sum of sinusoids has both first- and second-order components, but these components show qualitatively different dependences on spatial phase (Fig. 1). At one spatial phase, the "peak" spatial phase, the first-order responses are maximal (Fig. 1 A), with a peak amplitude of 40 impulses per second. When the grating is shifted by one-fourth of a period, the first-order response vanishes into the noise (Fig. 1 B). However, the second-order response remains unchanged from the "peak" spatial phase, over the entire range of temporal frequencies. Thus, with great precision, the second-order response is independent of the first-order response.

The spatial phase independence of the second-order response has an important implication for modelling the nonlinear pathway of the Y cell (Enroth-Cugell and Robson, 1966; Hochstein and Shapley, 1976 *b*, Victor et al., 1977). We discuss this implication here because it is necessary for the interpretation of later experiments. Spatial-phase independence implies that there must be a large number of distinct nonlinear pools. Consider instead the model of a single pool, whose output, after a nonlinear transformation, generates the second-order response of the Y cell. Then, shifting the spatial phase of the grating would alter the net modulation of light flux into the pool, and hence would alter the second-order response. To account for the spatial-phase invariance of the second-order response, it is necessary to postulate a large number of independent pools, the "subunits," each of whose outputs pass through a nonlinear transduction before contributing to the ganglion cell's response (Hochstein and Shapley, 1976 *b*). Such a receptive-field model is shown in Fig. 2. The nonlinear subunits are superimposed on the classical center and surround mechanisms, which generate the independent first-order response. The sensitivity profiles of the subunits are shown to be narrower than that of the center or surround mechanism, because the nonlinear response persists to higher spatial frequencies than does the first-order response (Hochstein and Shapley, 1976 *b*; Victor and Shapley, 1979). In any given position of the grating, about the same fraction of subunits will be maximally stimulated by the pattern's modulation. Because the light signal pooled by each subunit is postulated to undergo a nonlinear transformation, the subunit responses do not cancel each other out. Hence, the summed subunit response will be approximately constant as a function of spatial phase, despite variation of the first-order response from peak to null.

In principle, the number of such nonlinear subunits can be estimated by the fractional variation of the second-order kernels with spatial phase. Assume that the subunits are distributed in space randomly; then their spatial phases with respect to a stimulus grating will be distributed randomly. With this assumption, one can calculate that M subunits will produce a fractional

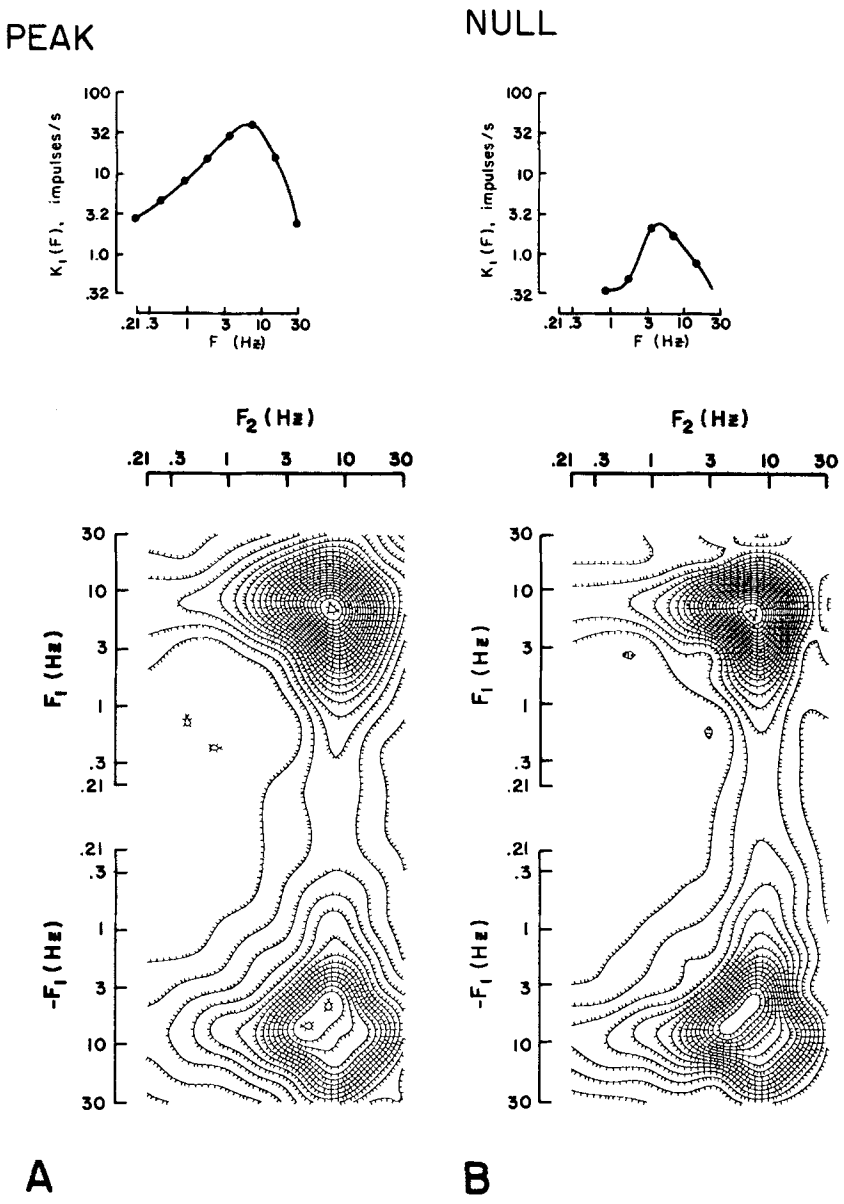

FIGURE 1. Dependence of first- and second-order response amplitudes of an on-center Y cell on spatial phase. The stimulus was a 0.1 cycle/deg grating, whose contrast was modulated by a sum of eight sinusoids. Each sinusoid produced a contrast of 0.05. (A) The grating produced a peak first-order response of 40 impulses/s. (B) The grating was shifted by one quarter of a spatial wavelength. The first-order response was 3 impulses/s or less, but the second-order response is virtually independent of spatial phase. Unit 13/14.

variation of $1/\sqrt{M}$ in the amplitude of the second-order frequency kernel, as spatial phase is varied. Our data show that the fractional variation of the second-order frequency kernel is ~ 0.1. Therefore, a rough estimate of the number of subunits M is 100. A more precise estimate would be influenced by error in the experimental determination of the second-order responses and the details of a model for the nonlinear transduction.

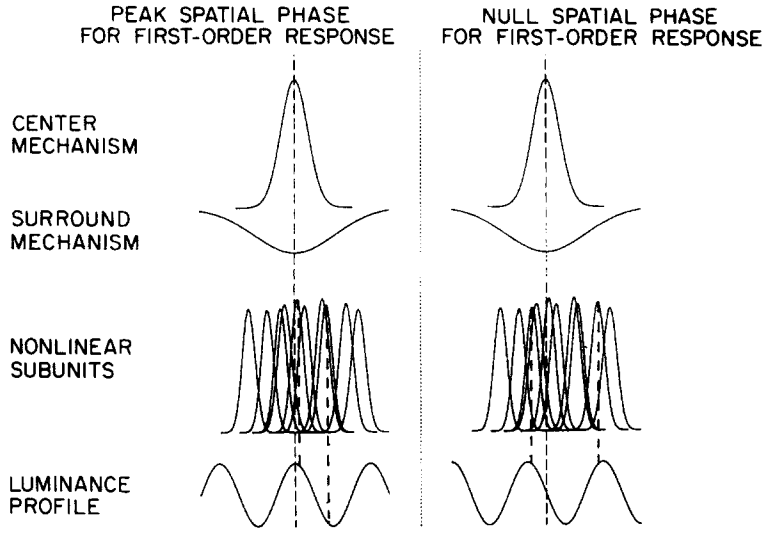

FIGURE 2. A receptive-field model that explains the spatial phase independence of the Y cell nonlinear response. Superimposed on a linear receptive-field model is an array of nonlinear subunits. Each subunit sums light linearly over its indicated spatial extent, but applies a nonlinear transduction to this signal. The outputs of the nonlinear subunits are summed to generate the nonlinear response of the Y cell. The linear and nonlinear responses are thus generated by independent pathways. A sine grating in any spatial phase has peaks that line up with some nonlinear subunits, and zero-crossings that line up with other nonlinear subunits. Thus, in any spatial phase, about the same fraction of nonlinear subunits are stimulated by contrast modulation of the grating. Therefore, the second-order response is independent of spatial phase. The sensitivity profiles of the nonlinear subunits are narrower than those of the center or surround mechanisms, to indicate their higher resolution.

Further evidence for the local generation of nonlinear responses can be obtained from experiments with localized stimuli. In Fig. 3, the response of a Y cell to a modulated bar is compared with the response to a grating whose lobes are comparable to the bar in width. The bar is positioned on the receptive-field center, so that a large first-order response is produced; the grating is positioned so that no first-order response is produced. The second-order responses to these two stimuli are nearly identical. Thus, the second-order response to a grating is not a result of interactions between distinct portions of the receptive field.

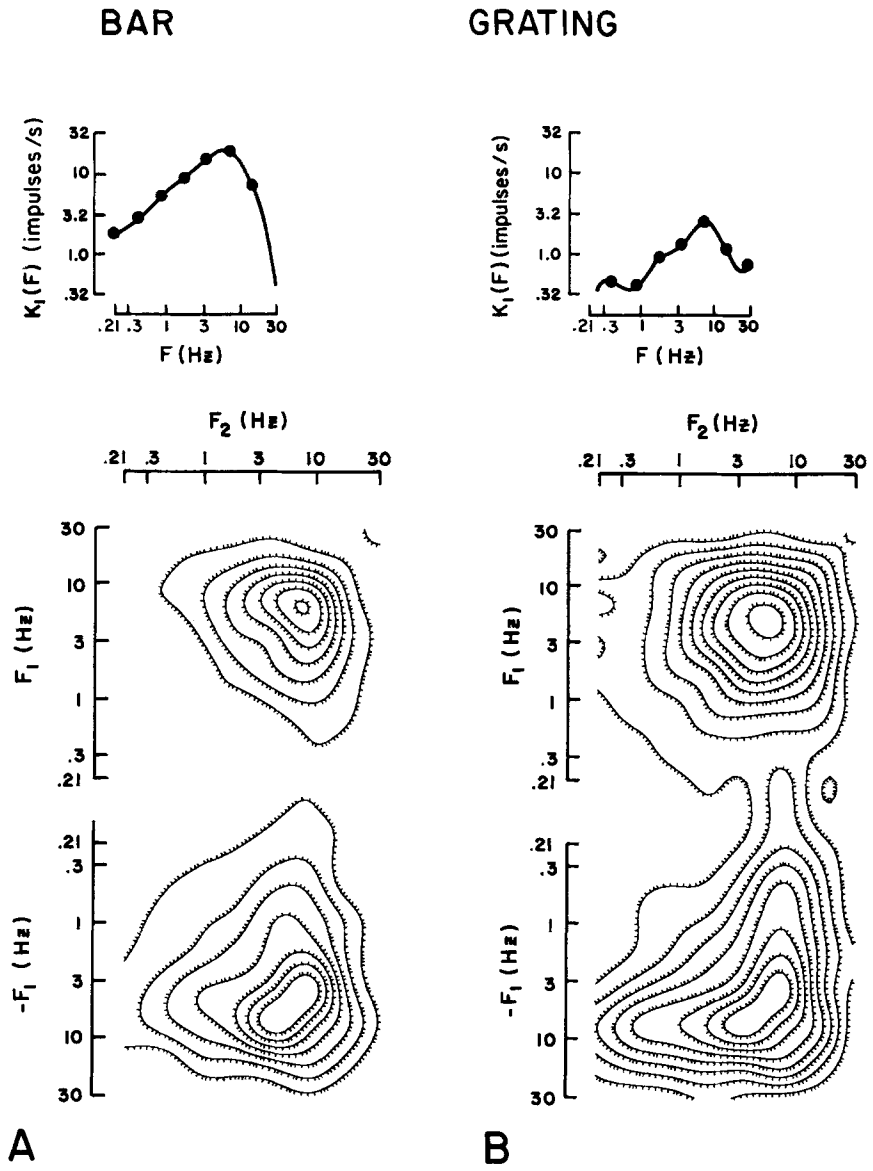

FIGURE 3. Comparison of responses of an on-center Y cell to a bar and a grating. (A) The stimulus was a 1.0° × 20° vertical bar, positioned over the receptive-field center. (B) The stimulus was an 0.6 cycle/deg grating, positioned near the null spatial phase for the first-order response. The contrast modulation signal was a sum of eight sinusoids, each producing a contrast of 0.05. Although the maximum first-order response varied from 17 impulses/s (bar) to 3 impulses/s (grating), the second-order responses were virtually identical. Unit 13/10.

Sandwich Model

The above experiments led to a model of the nonlinear pathway of the Y cell as an array of subunits, each of which sums light linearly over its extent. Each subunit then applies a static nonlinearity, and the outputs of the subunits are summed by the ganglion cell to give the observed second-order response. The dependence of the second-order frequency kernel $K_2(F_1, F_2)$ on the frequencies F_1 and F_2 (cf. Figs. 1, 3) implies that there must be significant dynamical components in the nonlinear pathway. In the sandwich model, the dynamics may be introduced into the subunits themselves (before the nonlinearity), or after pooling of the subunits' output, or at both points.

The linear pooling of light by a single subunit may be represented by a filter L_1, with transfer function $L_1(F)$. The summing of subunit responses may be represented by a second linear filter L_2, with transfer function $L_2(F)$. The predicted second-order frequency kernel of this linear/static nonlinear/linear transduction can be calculated by means of the relation of the frequency kernels to the Wiener kernels (Victor and Shapley, 1980):

$$K_2(F_1, F_2) \approx bL_1(F_1)L_1(F_2)L_2(F_1 + F_2). \tag{4}$$

The qualitative features of the data (e.g., Figs. 1 and 3) immediately imply that both L_1 and L_2 are nontrivial transductions. If L_1 were absent, the second-order kernel (Eq. 4) would be a function only of $F_1 + F_2$. But the presence of distinct peaks in both the sum and difference regions shows that $K_2(F_1, F_2)$ is large only when neither frequency F_1 or F_2 is very close to zero. The presence of distinct peaks thus reflects the tuning of the filter within the subunit, L_1.

Alternatively, if L_2 were absent, then

$$\begin{aligned} |K_2(F_1, F_2)| &\approx b\,|L_1(F_1)|\,|L_1(F_2)| \\ &= b\,|L_1(F_1)|\,|\overline{L_1(F_2)}| \\ &= b\,|L_1(F_1)\cdot L_1(-F_2)| \\ &\approx |K_2(F_1, -F_2)|, \end{aligned} \tag{5}$$

which states that the amplitudes of the sum frequencies $F_1 + F_2$ would be equal to the amplitudes of the corresponding difference frequencies $F_1 - F_2$. However, experimentally, this summetry between the sum and difference regions is consistently broken. The peak in the difference region usually has a smaller amplitude than the peak in the sum region. In many cells the peak in the difference frequency region occurs at a higher input temporal frequency than the peak in the sum frequency region. This suggests that L_2, the linear transduction which follows the static nonlinearity, has a gentle high-pass characteristic.

These qualitative statements can be made rigorous and quantitative by fitting functional forms for $L_1(F)$ and $L_2(F)$. This procedure is carried out in Fig. 4 with data from a typical on-center Y cell (Fig. 4 A). We fit the sandwich model to the data by determining amplitudes and phases of L_1 and LL_2 at a mesh of 20 frequencies equally spaced on a linear scale. The criterion for best

fit was the minimum-squared difference between the amplitudes and phases predicted by Eq. 4 and the amplitudes and phases derived from the empirical second-order kernels. The fitted amplitudes $|L_1(F)|$ and $|L_2(F)|$ are shown in Fig. 4 C, and have the characteristics expected from the qualitative

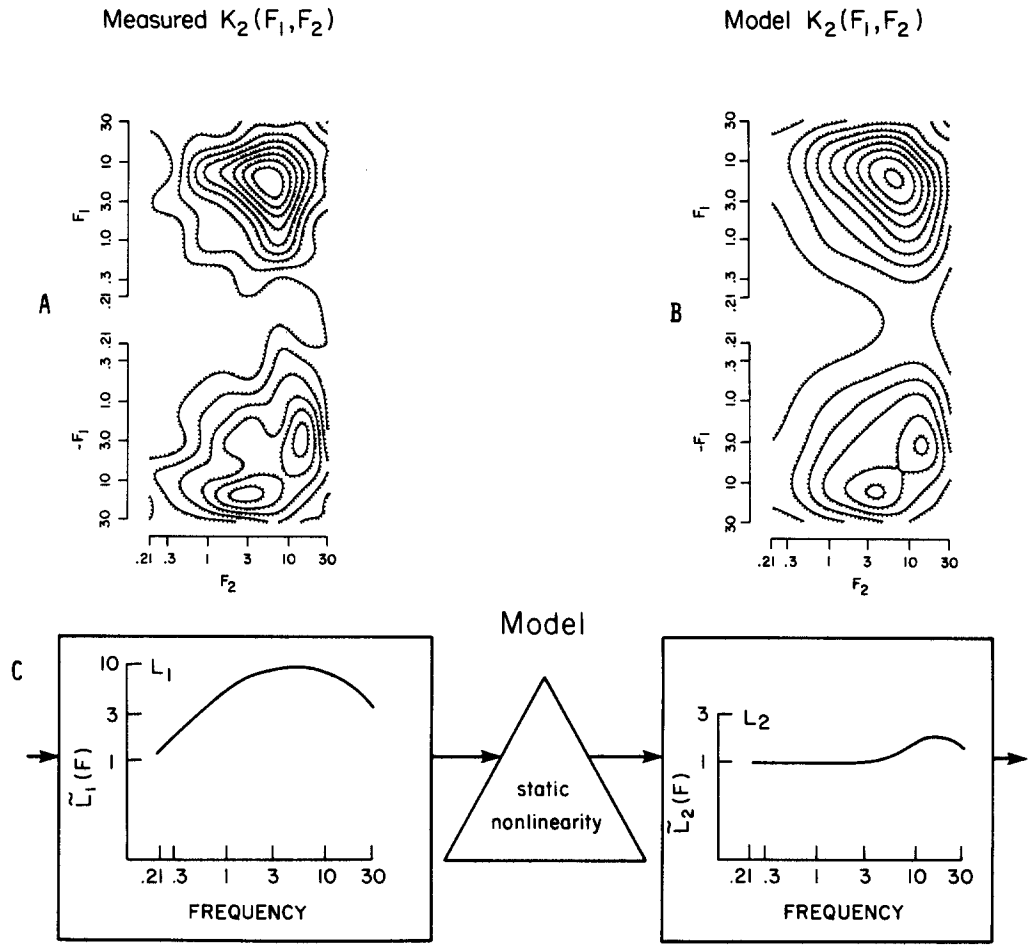

FIGURE 4. The sandwich model for the nonlinear pathway of the Y cell. (A) The second-order response of an on-center Y cell to an 0.25 cycle/deg grating positioned to elicit no first-order response is shown. The contrast of the grating was modulated by a sum of eight sinusoids, each producing a contrast of 0.05. (B) The second-order frequency kernel amplitudes of a model transducer consisting of a linear transducer L_1, followed by a static nonlinearity, followed by a second linear transducer, L_2. (C) The amplitudes of the transfer functions $L_1(f)$ and $L_2(f)$. These amplitudes were chosen to maximize the agreement between the measured frequency kernel and the model values. Unit 14/15.

discussion above. L_1 is bandpass and L_2 is a gentle, higher-pass filter. The phases of $L_1(f)$ and $L_2(f)$ are not uniquely determined, because the effects of delay before or after the nonlinearity are indistinguishable. Aside from this

ambiguity, the phase data are consistent with the idea that L_1 and L_2 are causal transductions.

The second-order frequency response of the model Fig. 4 B, corresponds closely to that of the data. The discrepancy between the measured values $K_2(f_i, \pm f_j)$ and the values predicted Eq. 4 from the fitted values $L_1(F)$ and $L_2(F)$ averages <1 impulse/s. The major peaks in the sum regions and the difference regions are at about the same input frequencies, and have the same heights and breadths. Thus, the linear/static nonlinear/linear transduction is a good initial description of the dynamics of the nonlinear response.

Nature of the Nonlinearity

The above analysis of the shape of the second-order frequency kernel yielded nformation on the dynamics of the two linear filters of the sandwich model. An analysis of the overall size of the second-order response, as a function of the contrast of the visual stimulus, provides information on the static nonlinear element N.

The root-mean-squared average of the second-harmonic components $K_2(F, F)$ is a convenient index of the strength of the nonlinear response. The dependence of this index on contrast of a grating stimulus is shown in Fig. 5.

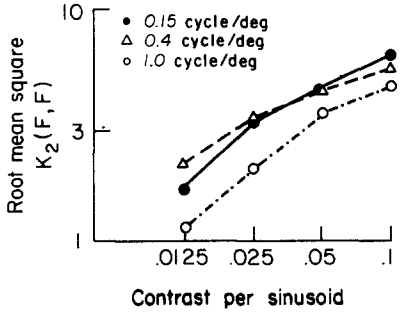

FIGURE 5. The dependence of total second-order responses, as measured by the root mean square $K_2(F, F)$, on the contrast of a spatial sine grating. The abscissa indicates the contrast per sinusoid of the eight-sinusoid sum that provided the temporal modulation for the pattern stimulus. Unit 22/13.

As input contrast increases, the strength of the second-order response grows at first proportionally, and then more slowly. This dependence can be interpreted by comparison with the predicted behavior of a static nonlinearity such as $N(x) = |x|^{\alpha}$. The amplitude vs. response of such a device is graphed in Fig. 6. Such a nonlinearity may be called a symmetric rectifier with a power law characteristic. For such a transducer, the curves in Fig. 5 of log response amplitude vs. log input amplitude would be straight lines with slope equal to the exponent α. Thus, Fig. 5 indicates that for low contrast, the nonlinearity of the cat retina resembles such a rectifier. At higher contrasts, there seems to be a saturation in the nonlinearity. (The odd-order components of the nonlinearity in the cat retina cannot be determined from responses to the grating stimulus, since the effects of the excursions above background are cancelled by the effects of the excursions below background. This problem is

not avoided by using a stimulus such as a spot or bar, because of the linear mechanisms that overlap the nonlinear mechanism in space.)

Further evidence that the static nonlinearity in the retina resembles a rectifier can be obtained from an analysis of higher-order components of the response. The method of variation of input phase suffices to isolate all 344 third-order components and 1,408 fourth-order components. In order to get more precise data, in some experiments the standard experimental protocol was repeated eight times to improve the signal-to-noise ratio. The individual components of the higher-order frequency kernels are too small to permit a detailed analysis. However, useful information is present in the total power present at each order of nonlinearity.

Table I shows the total power present at the first four orders in the response of an on-center Y cell. The data were obtained using a 0.75 cycles/deg grating that elicited a small first-order response (Victor and Shapley, 1979). This is manifest in the total first-order power, which increases by a factor of 3.81 as

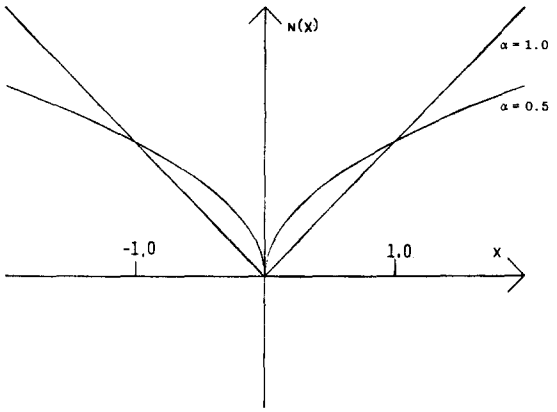

FIGURE 6. Amplitude response characteristic for two sorts of symmetric power law rectifiers. These obey the relation $N(x) = |x|^{\alpha}$. The characteristics of two such rectifiers, with $\alpha = 1$ and $\alpha = 0.5$ are shown. The retinal nonlinearity seems to be approximated best by a rectifier with $\alpha \cong 0.9$.

input contrast is doubled (a precisely linear transduction would show a fourfold increase). The total power in the third-order components probably is entirely due to noise, because it is independent of input contrast and represents very small Fourier coefficients ($\lesssim 0.2$ impulses/s on average).

The even-order components reflect characterizations of the nonlinearity. The presence of substantial fourth-order components at low levels of input contrast supports the notion that the nonlinearity is similar to a rectifier of some kind. The second- and fourth-order powers increase by approximately the same factor, 3.04 and 3.08, as contrast doubles. This power ratio corresponds to an amplitude ratio of ~ 1.75 ($\approx \sqrt{3.06}$). A power law rectifier $N(x) = |x|^{\alpha}$ would show this behavior for $\alpha = 0.87$. Thus, the notion that the nonlinearity resembles a power law rectifier is supported by the scaling behavior of the second-order frequency kernel and the overall power of the fourth-order responses.

Dependence on Spatial Frequency

The second-order frequency kernels of Y cells show a consistent pattern of dependence on the spatial frequency of the grating used to elicit the response. Fig. 7 shows the amplitudes of the second-order frequency kernels obtained from an on-center Y cell at two spatial frequencies. The amplitudes of high temporal frequency components increase with decreasing spatial frequency. The amplitudes of low temporal frequency components increase more slowly with decreasing spatial frequency and often show an optimum at an intermediate frequency. As a consequence of these spatial changes, the second-order responses shift to higher temporal frequency with lower spatial frequency.

The sandwich model (Eq. 4) is useful in analyzing this spatiotemporal coupling. A priori, the site of the spatiotemporal coupling of the second-order kernel might be either L_1 or L_2 or both filters in the sandwich. One can

TABLE I
TOTAL RESPONSE POWER OF DIFFERENT ORDERS OF RESPONSE

	Contrast per sinusoid	
Order	0.025	0.05
	$(impulses/s)^2$	
1	4.7	17.9
2	198.5	602.5
3	8.2	9.5
4	49.2	151.6

Response power of a cat Y cell in response to a sine grating, amplitude-modulated in time by a sum of sinusoids. The stimulus grating had a spatial frequency high enough so that the first-order responses were small. First-order, second-order, third-order, and fourth-order responses were calculated by Fourier transforming the impulse train of the ganglion cell. Response power was calculated as the sum of the squares of the response amplitudes at each of the output frequencies appropriate for that order.

evaluate the contrasting hypotheses that L_1 alone, or that L_2 alone, is responsible for the spatiotemporal coupling on the basis of qualitative features of the data. The first step in this procedure is to compare sensitivities as a function of spatial frequency, rather than absolute response sizes. Sensitivity is defined here as the reciprocal of contrast necessary for a criterion value of 2 impulses per second. By using a low criterion, responses at different spatial frequencies are compared at near-threshold contrasts. This is an attempt to minimize the confounding effects of the contrast gain control (Shapley and Victor, 1979).

One can dissect apart the spatiotemporal coupling of the two filters in the sandwich model. This is done by choosing to study the spatial frequency dependence of second-order components which occur at almost identical output frequencies. If spatiotemporal coupling is observed in such components, it must be due to the filter before the nonlinearity, L_1. Any spatiotemporal coupling in L_2 will not be revealed by comparing nearly identical output

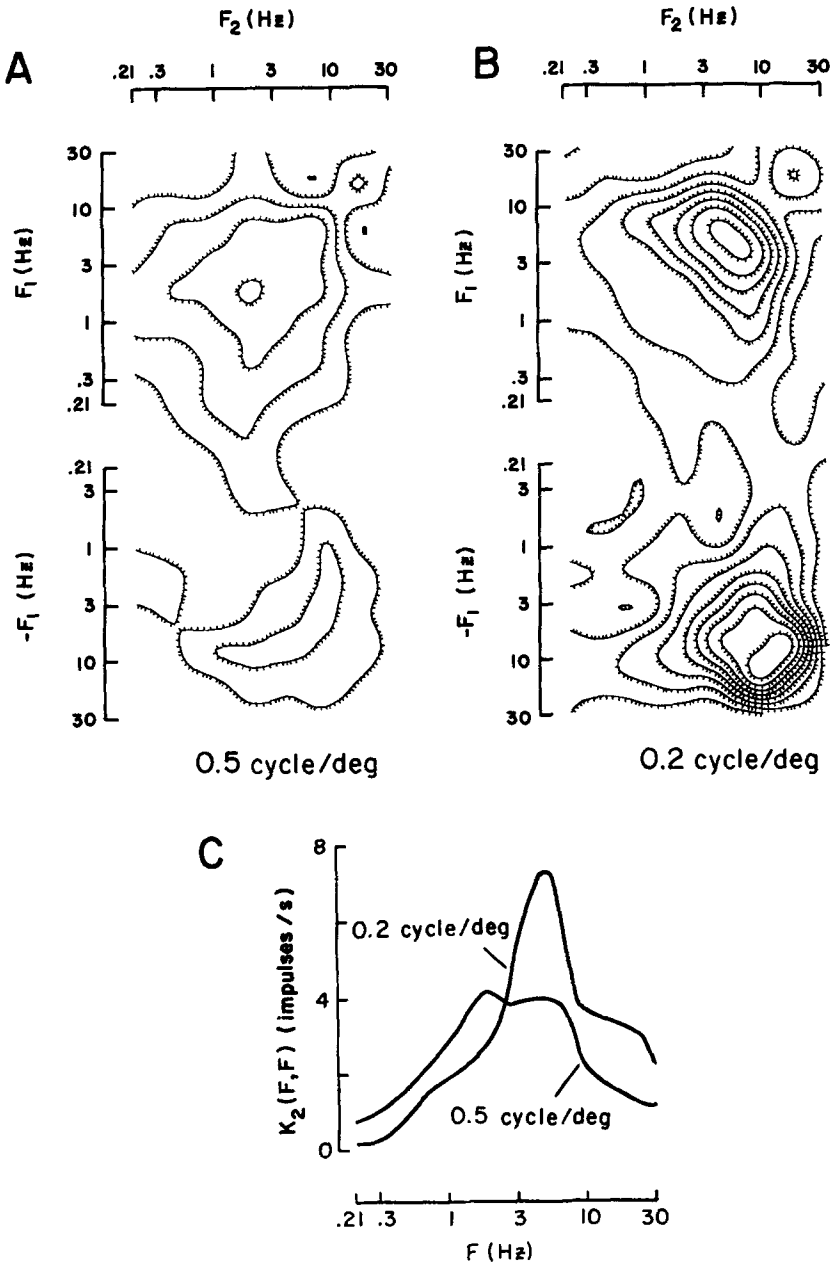

FIGURE 7. Amplitudes of the second-order frequency kernel of an on-center Y cell as a function of spatial frequency. (A) 0.5 cycle/deg; (B) 0.2 cycle/deg. Each grating was positioned to elicit a maximal first-order response, and each component of the eight-sinusoid sum generated a contrast of 0.025. (C) Slices of the second-order frequency kernels along the diagonal of pure second harmonics are shown. A shift to higher temporal frequencies at lower spatial frequencies is evident. Unit 28/2.

frequencies. Data chosen for such a comparison are shown in Fig. 8. This figure shows a plot of some second-order sensitivities as a function of spatial frequency for the on-center Y cell of Fig. 7. The two components K_2 (1.9, 1.9) and K_2 (7.8, −3.9) have nearly identical output frequencies: the respective sum and difference frequencies differ by 0.06 Hz. Yet the sensitivities of these two components display a remarkable difference in their spatial-frequency dependence. The source of this difference must reside in L_1, which acts on the input frequencies. One may use similar reasoning to isolate the spatiotemporal

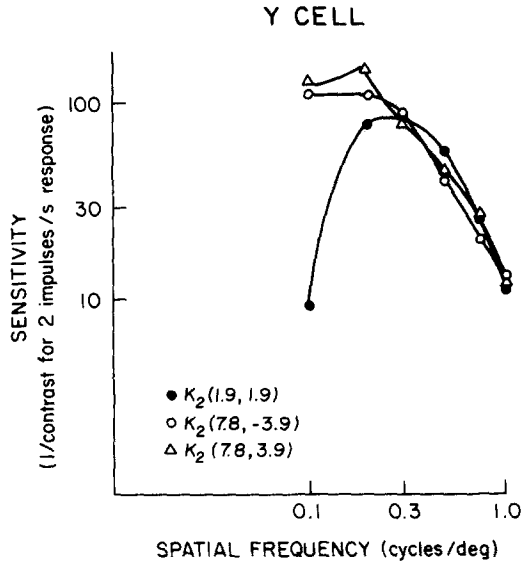

FIGURE 8. Sensitivities of components of the second-order frequency kernel of an on-center Y cell as a function of spatial frequency. At each spatial frequency, a sine grating was positioned to produce a minimal first-order response. The contrast of the grating was modulated by a series of eight-sinusoid signals, at a range of contrasts per sinusoid. Sensitivity was determined as the reciprocal of the contrast that gave a criterion second-order response amplitude of 2 impulses/s. Sensitivities were calculated at the lattice points (1.9, 1.9) (●); (7.8, -3.9) (○); and (7.8, 3.9) (△). The dependence of sensitivity on spatial frequency depends primarily on the input frequencies, rather than the output frequencies. Unit 28/2.

coupling in L_2, the filter after the nonlinearity. Here it suffices to compare the spatial frequency dependence of a sum frequency with the corresponding difference frequency. In such a case the input frequencies are exactly identical, but the output frequencies are widely different. For example, the two components K_2 (7.8, 3.9) and K_2 (7.8, −3.9) have equal input frequencies, yet output frequencies that differ by a factor of 3. These sensitivities, however, behave similarly as a function of spatial frequency. In general, the spatial frequency dependence of a component $K_2(f_i, \pm f_j)$ depends on the input temporal frequencies f_i and f_j more strongly than on the output temporal

frequency $f_i \pm f_j$. Thus the first filter of the sandwich model, L_1, is the primary determinant of spatiotemporal coupling.

The quantitative amount of spatiotemporal coupling varies across the population of Y cells. For instance, in some cells the values of $K_2(7.8, \pm 3.9)$ decline at low spatial frequencies, which is unlike the behavior of the cell in Fig. 8. However, in every case $|K_2\ (1.9, 1.9)|$ declines more at low spatial frequency than do $|K_2\ (7.8, \pm 3.9)|$. The decline of the second-order amplitudes at low spatial frequency suggests that there is a center-surround organization in L_1, the prefilter in the sandwich model.

Elevation of Mean Rate

There is another characteristic nonlinear feature of the responses of Y cells which we can relate to the second-order frequency responses and to the "sandwich" model of the nonlinear pathway. This characteristic is the elevation of the mean rate in the presence of a spatial pattern modulated in time. This effect was first noted in the Y cell responses to drifting grating patterns (Enroth-Cugell and Robson, 1966; Cleland et al. 1971). It is noticeable also in the responses of Y cells to sine gratings modulated by a sum of sinusoids. Typical data on the elevation of mean rate with contrast are shown in Fig. 9

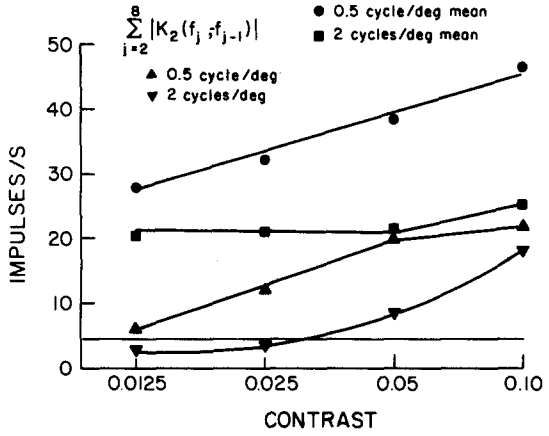

FIGURE 9. Elevation of mean rate with contrast. The mean rate of an on-center Y cell is plotted as a function of contrast. The results from two different experimental runs at two different spatial frequencies are shown: those for 0.5 cycle/deg (●) and 2 cycles/deg (■). The 0.5 cycle/deg grating was placed at the null position for first-order responses. At 2 cycles/deg there were no first-order responses, only second-order responses. Also plotted in the figure are the sums

$$\sum_{j=2}^{8} |K_2(f_j, -f_{j-1})|$$

which are a rough estimate of the contribution of the second-order nonlinear interaction to the elevation of the mean. These sums are shown for 0.5 cycle/deg (▲) and 2 cycles/deg (▼). The thin horizontal line indicates the standard error for the sums of the second-order responses. Unit 29/32.

for one on-center Y cell. The circles are the mean rates for a 0.5 cycle/deg grating positioned so that it elicited essentially no first-order responses. The squares are mean rates in the same cell in response to a 2 cycles/deg grating. This spatial frequency was near the spatial resolution limit of the cell and again there were no first-order responses. One sees that the mean rate increased with increasing contrast at 0.5 cycle/deg, and that the mean rate was roughly constant up to 0.05 contrast at 2 cycles/deg and then increased between 0.05 and 0.1 contrast.

We have observed that the elevation of the mean rate is highly correlated with the total strength of the second-order frequency response. This suggests that the elevation of the mean is caused by the same nonlinearity which produces the second harmonics and intermodulation components in the modulated response. We can check the consistency of this notion quantitatively. Suppose all the nonlinear responses are produced by a linear/nonlinear/linear sandwich in which the static nonlinearity is a rectifier $N(x) = |x|^{\alpha}$. Then one can show that the elevation of the mean should be

$$K_0 = \frac{1}{\alpha} \sum_{j=1}^{8} K_2(f_j, -f_j)$$

in the case of temporal modulation by a sum of eight sinusoids. Unfortunately, we cannot measure the set of $K_2(f_j, -f_j)$ separately because they all occur at the same output frequency, namely zero frequency. But we can estimate roughly how large they are by considering the nearby components $K_2(f_j, -f,za_{-1})$. The sums

$$\sum_{j=2}^{8} |K_2(f_j, -f_{j-1})|$$

are graphed in Fig. 9 for 0.5 cycle/deg as triangles, and for 2 cycles/deg as inverted triangles. The standard error of the mean of the sum is drawn in to indicate when the sum is significantly out of the noise. Clearly, the increase in these difference-frequency components with contrast parallels the elevation of mean rate. At the high spatial frequency the mean only rises when the sum of the kernel amplitudes climbs out of the noise. The mean rate of 0.5 cycle/deg rises uniformly as does the sum of the $|K_2(f_j, -f_{j-1})|$. In fact, the approximately parallel slopes of the mean and the sum of the kernel amplitudes at $(f_j, -f_{j-1})$ implies that the value of the exponent α is close to 1.

The mean rate data imply one further deduction, about the postfilter L_2 in the sandwich model. If L_2 went to zero at zero frequency, there would be no elevation of the mean though there were significant second-order responses at higher output frequencies. Thus, the elevation of the mean confirms our earlier inferences that L_2 is more or less flat from zero frequency up to some intermediate frequency and then has a gentle high-pass characteristic. Both the estimate of the contrast dependence of the nonlinearity and inferences about the characteristics of the postfilter of the sandwich model are confirmed by the results on the elevation of the mean rate.

It should be noted that X ganglion cells have almost zero second-order frequency responses over the range in contrast from 0.0125 up to 0.10, and over this same range the mean rate is almost unaffected by modulation of pattern contrast.

DISCUSSION

We have proposed a linear/nonlinear/linear model for the nonlinear pathway of the Y ganglion cells of the cat retina. This model accounts for the major features of the second-order nonlinear response of the Y cell, and for the elevation of the mean rate of Y cells with contrast. The nonlinear pathway is composed of an array of spatial subunits. Within each subunit, signals from photoreceptors are pooled by a mechanism with a center-surround organization.

The subunit response passes through a static nonlinearity, whose operating curve is like a rectifier with a sharp corner. The output of many such subunits distributed over a wide area is pooled by a second filter, L_2, to generate the nonlinear components of the Y cell response. The second filter, L_2, must have gentle bandpass or highpass characteristics in order to explain the asymmetry between the sum and difference regions (Figs. 1 and 3), of the second-order frequency kernel.

Anatomical Basis for the Y Cell Nonlinear Pathway

Our model for the nonlinear pathway of the Y cell suggests some correlations with the retinal anatomy. We propose that the subunits of the Y cell correspond to the bipolar cells, that the nonlinearity is generated at the amacrine cell layer (Toyoda, 1974; Naka et al., 1975), and that amacrine cells are also responsible for the pooling of subunit signals. Evidence for this correspondence is drawn from the present physiological studies and direct investigations of the properties of interneurons in retinas of lower vertebrates.

One can rule out the photoreceptors as the source of any of the nonlinearity seen in Y cells, for two separate reasons. First, X cells receive input from the same kind of photoreceptors as Y cells, but show little if any of the second-order responses so characteristic of Y cells (Hochstein and Shapley, 1976 *a*; Victor et al., 1977; Victor and Shapley, 1979). Second, over the range of contrasts used here (0.05–0.2 rms contrast), the saturation seen in the second-order responses of Y cells is observed neither in the first-order responses of Y cells nor in the first-order responses of X cells (cf. Table I; Shapley and Victor, 1978). A photoreceptor nonlinearity would affect all the responses of the ganglion cells.

The model for the nonlinear pathway of the Y cell requires that the subunit has center-surround organization. In the goldfish (Kaneko, 1970, 1971), the carp (Toyoda, 1974; Famiglietti et al., 1977), the catfish (Naka et al., 1975), and the mudpuppy (Werblin and Dowling, 1969; Dowling, 1970), the bipolar cell is the first neuron encountered which has an antagonistic center-surround organization. In the cat, the spatial and temporal properties of the subunit, as

inferred from the sandwich model, closely resemble the spatial and temporal properties of the X cell linear receptive-field mechanisms (Victor and Shapley, 1979; So and Shapley, 1979). Thus, it is likely that the bipolar cell is the anatomical substrate of both the subunit of the Y cell and the center-surround organization of the X cell.

In the retinae of lower vertebrates, the bipolar responses are qualitatively linear, whereas some amacrine cell responses are qualitatively nonlinear (Werblin and Dowling, 1969; Dowling, 1970; Kaneko, 1970, 1971; Toyoda et al., 1973; Toyoda, 1974; Naka et al., 1975). This supports the idea that the nonlinearity resides in an amacrine cell. If the subunit nonlinearity resides in the amacrine cell layer, then so must the pooling of subunit responses over wide regions. Some amacrine cells of the cat have wide dendritic spread (Gallego, 1971) and there are many amacrine-amacrine synapses (Kolb and Famiglietti, 1974). Our hypotheses about the amacrine cells demand great heterogeneity among amacrine cell types; this is consistent with present ideas about the morphology and physiology of these cells.

Rigorous proof of the above correspondence requires more than input-output studies of the cat retina; the properties of cat retinal interneurons themselves must be investigated. We hope that these hypotheses are a stimulus for such experiments. However, from the point of view of one interested in the visual system as a whole, the value of the sandwich model as a functional description of the Y cell pathways is independent of our hypotheses concerning the correspondence of elements of the model with retinal interneurons.

We wish to thank Dr. William Scott of Hoffmann-La Roche, Inc. for his generous gift of diallylbis-(nortoxiferine).

This work was supported by research grants EY-1472, EY-1428, EY-188, and GM-1789 from the National Institutes of Health. Dr. Shapley was supported by a Research Career Development Award from the National Eye Institute.

Received for publication 22 May 1979.

REFERENCES

AHLBERG, J. H., G. N. NILSON, and J. L. WALSH. 1967. The Theory of Splines and Their Applications. Academic Press, Inc., New York. Chapter 7. 235–264.

CLELAND, B. G., M. W. DUBIN, and W. R. LEVICK. 1971. Sustained and transient neurones in the cat's retina and lateral geniculate nucleus. *J. Physiol. (Lond.).* **217:** 473–496.

DOWLING, J. E. 1970. Organization of vertebrate retinas. *Invest. Ophthalmol.* **9:** 655–680.

ENROTH-CUGELL, C., and J. G. ROBSON. 1966. The contrast sensitivity of retinal ganglion cells of the cat. *J. Physiol. (Lond.).* **187:** 517–552.

FAMIGLIETTI, E. V., JR., A. KANEKO, and M. TACHIBANA. 1977. Neuronal architecture of on and off pathways in ganglion cell in carp retina. *Science (Wash. D.C.)* **198:** 1267–1269.

GALLEGO, A. 1971. Horizontal and amacrine cells in the mammal's retina. *Vision Res.* **11** (Suppl. 3): 33–50.

HOCHSTEIN, S., and R. M. SHAPLEY. 1976 *a*. Quantitative analysis of retinal ganglion cell classifications, *J. Physiol. (Lond.).* **262:** 237–264.

HOCHSTEIN, S., and R. M. SHAPLEY. 1976 *b*. Linear and nonlinear spatial subunits in Y cat retinal ganglion cells. *J. Physiol. (Lond.).* **262:** 265–284.

KANEKO, A. 1970. Physiological and morphological identification of horizontal, bipolar, and amacrine cells in the goldfish retina, *J. Physiol. (Lond.)*. **207:** 623–633.

KANEKO, A. 1971. Physiological studies of single retinal cells and their morphological identification. *Vision Res.* **11** (Suppl. 3): 17–26.

KOLB, H., and E. V. FAMIGLIETTI, JR. 1974. Rod and cone pathways in the inner plexiform layer of cat retina. *Science (Wash. D.C.)* **186:** 47–49.

NAKA, K-I., P. Z. MARMARELIS, and R. Y. CHAN. 1975. Morphological and functional identification of catfish retinal neurons. III. Function identification. *J. Neurophysiol.* **38:** 92–131.

SHAPLEY, R. M., and M. ROSSETTO. 1976. An electronic visual stimulator. *Behav. Res. Methods Instrum.* **8:** 15–20.

SHAPLEY, R. M., and J. D. VICTOR. 1978. The effect of contrast on the transfer properties of cat retinal ganglion cells. *J. Physiol. (Lond.)*. **285:** 275–298.

SHAPLEY, R. M., and J. D. VICTOR. 1979. The contrast gain control of the cat retina. *Vision Res.* **19:** 431–434.

SO, Y. T. and R. M. SHAPLEY. 1979. Spatial properties of X and Y cells in lateral geniculate nucleus of the cat and conduction velocities of their inputs. *Exp. Brain. Res.* **36:** 533–550.

SPEKREIJSE, H. 1969. Retification in the goldfish retina: analysis by sinusoidal and auxiliary stimulation. *Vision Res.* **9:** 1461–1472.

TOYODA, J-I. 1974. Frequency characteristics of retinal neurons in the carp. *J. Gen. Physiol.* **63:** 214–234.

TOYODA, J-I., H. HASHIMOTO, AND K. OHTSU. 1973. Bipolar-amacrine transmission in the carp retina. *Vision Res.* **13:** 295–307.

VICTOR, J. D., and B. W. KNIGHT. 1979. Nonlinear analysis with an arbitrary stimulus ensemble. *Q. Appl. Math.* **37:** 113–136.

VICTOR, J. D., and R. M. SHAPLEY. 1979. Receptive-field mechanisms of cat X and Y retinal ganglion cells, *J. Gen. Physiol.* **74:** 275–298.

VICTOR, J. D., and R. M. SHAPLEY. 1980. A method of nonlinear analysis in the frequency domain. *Biophysical J.* In press.

VICTOR, J. D., R. M. SHAPLEY, and B. W. KNIGHT. 1977. Nonlinear analysis of retinal ganglion cells in the frequency domain. *Proc. Natl. Acad. Sci. U.S.A.* **74:** 3068–3072.

WERBLIN, F. S., and J. E. DOWLING. 1969. Organization of the retina of the mudpuppy, *Necturus maculosus*. II. Intracellular recording. *J. Neurophysiol.* **32:** 339–355.